Journal of Systems Engineering and Electronics
Vol. 30, No. 1, February 2019, pp.57 – 67

Labeled box-particle CPHD filter for multiple extended targets tracking

ZOU Zhibin, SONG Liping*, and CHENG Xuan

School of Electronic Engineering, Xidian University, Xi'an 710071, China

Abstract: In multiple extended targets tracking, replacing traditional multiple measurements with a rectangular region of the non-zero volume in the state space inspired by the box-particle idea is exactly suitable to deal with extended targets, without distinguishing the measurements originating from the true targets or clutter. Based on our recent work on extended box-particle probability hypothesis density (ET-BP-PHD) filter, we propose the extended labeled box-particle cardinalized probability hypothesis density (ET-LBP-CPHD) filter, which relaxes the Poisson assumptions of the extended target probability hypothesis density (PHD) filter in target numbers, and propagates not only the intensity function but also cardinality distribution. Moreover, it provides the identity of individual target by adding labels to box-particles. The proposed filter can improve the precision of estimating target number meanwhile achieve targets' tracks. The effectiveness and reliability of the proposed algorithm are verified by the simulation results.

Keywords: extended target, multiple targets tracking, labled box-particle, cardinalized probability hypothesis density (CPHD).

DOI: 10.21629/JSEE.2019.01.06

1. Introduction

With the development of advanced sensor technologies, such as phased array radar and inverse synthetic aperture radar (ISAR), each moving target may occupy multiple range resolution cells. Targets that potentially give rise to more than one measurement per time step are denoted as extended targets. Real-time tracking of extended targets is becoming more and more important in modern tracking systems, since the targets can provide not only the kinematic state but also their extent. Gilholm and Salmond [1] presented a spatial distribution model for tracking extended targets under the assumption that the number of target-related measurements per time step is Poisson distributed. Combining with the spatial distribution model aforementioned and finite set statistics (FISST) [2], Mahler put forward the so-called probability hypothesis density (PHD) filter for tracking extended targets [3], which can effectively avoid the combinatorial problem that arises from data association between multiple targets and multiple measurements. Then the Gaussian mixture implementation of the extended target PHD (ET-GM-PHD) was given by Granstrom et al. [4], on the assumptions that both target dynamics model and measurement model are linear Gaussian, and the numbers of measurements also follow the Poisson distribution. Furthermore, Orguner et al. brought forward the cardinalized PHD filter for extended target tracking (ET-CPHD) and its Gaussian implementation [5,6].

The box-particle filter (BPF), first proposed in [7], utilizes the interval analysis framework [8] to propagate weighted box-particles. As a generalized particle filter, the BPF could effectively deal with the measurements affected by three sources of uncertainty: stochastic, set-theoretic and data association uncertainty [9]. In many real applications, due to non-white and biased measurements, standard particle filter may achieve accurate and reliable performance by using thousands of particles, while the BPF could reach the similar level of accuracy with just a few dozen box-particles. Taking into account the advantages of reduced computational complexity and applicability with interval measurements for BPF, Schikora et al. [10,11] gave the BPF realization of PHD filter, and the BPF realization of cardinality balanced multi-target multi-Bernoulli filter was presented [12]. Besides, applying BPF framework to extended target tracking, Petrov et al. further developed ET-BPF [13,14] and its applications [15,16].

Along with the deep-going research, a PHD filter for tracking multiple extended targets was proposed by using interval analysis resulting from the GM-PHD filter and BPF [17]. Our recent work [17] on the box-particle PHD filter for extended target (ET-BP-PHD) simply needs to determine the rectangular spatial region of the expanding measurements, without distinguishing the measurements originating from the true targets or clutters. In case of

Manuscript received January 24, 2018.
*Corresponding author.

multiple extended targets, the certain ability of the anti-clutter seems to be one of the advantages of BP-PHD filter compared to the ET-PHD filter. On the other hand, the box-particle CPHD (BP-CPHD) filter [18] shows that the BP-CPHD filter can inherit the advantages of CPHD filter [19,20] that loosens the Poisson assumption of the PHD filter in target number and achieve more accurate target number estimation. Considering the superiority of CPHD filter in number estimation, applying the BP-CPHD filter [18] to extended target tracking would be a promising idea. However, measurements and states in random finite sets (RFSs) are in disorder, traditional PHD and CPHD filters based on RFS cannot recognize the correspondence between the current state and the previous state, therefore cannot identify different target tracks. Some approaches [21,22] are proposed to differentiate tracks by adding labels to particles.

In this paper, we propose a labeled box-particle CPHD filter in context of multiple extended targets (ET-LBP-CPHD) tracking with a varying number of targets, clutters and false alarms. The comparison between the proposed filter and the ET-BP-PHD filter is carried out, using the optical subpattern assignment (OSPA) metric for performance measure. The ET-LBP-CPHD filter, however, is demonstrated to be more precise in estimating number of targets and can distinguish different tracks.

The rest of the paper is structured as follows. The formal description of the extended target tracking problem is given in Section 2. Section 3 introduces the elements of the interval analysis and the BPF. The key idea of the labeled box-particle filter and the details of the proposed ET-LBP-CPHD filter implementation for multiple extended targets tracking are shown in Section 4. Numerical studies are presented in Section 5. Finally, conclusions are drawn in Section 6.

2. Extended target tracking problem

The system dynamic model and sensor measurement model of the nonlinear discrete-time system have the following general form:

$$\boldsymbol{x}_k = f(\boldsymbol{x}_{k-1}, u_{k-1}) \tag{1}$$

$$\boldsymbol{z}_k = h(\boldsymbol{x}_k, \upsilon_k) \tag{2}$$

where u_{k-1} and υ_k are the system noise and measurement noise respectively. The system transition function $f(\cdot)$ and the measurement function $h(\cdot)$ are both non-linear. In case of multiple extended targets, the multi-targets state set $\boldsymbol{X}_k$ is modelled as an RFS $\boldsymbol{X}_k = \{\boldsymbol{x}_k^1, \boldsymbol{x}_k^2, \ldots, \boldsymbol{x}_k^{N_k^T}\}$ where the states are $\boldsymbol{x}_k^j \in \mathbf{R}^{n_x}$ $(j = 1, \ldots, N_k^T)$ analogously. We define the measurement RFS $\boldsymbol{Z}_k = \{\boldsymbol{z}_k^1, \boldsymbol{z}_k^2, \ldots, \boldsymbol{z}_k^{N_k^z}\}$, $\boldsymbol{z}_k^i \in \mathbf{R}^{n_z}$ $(i = 1, \ldots, N_k^z)$, with both the number of targets N_k^T and the number of measurements N_k^z following Poisson distribution [1].

As the assumptions presented by Mahler [3], suppose that we are solving a 2-D extended target tracking scenario (x, y), the dynamic of an extended target could be simplified to the motion of its center of mass when its extension is not what we concern. The kinematic state-set $\boldsymbol{x}_k = (x_k, \dot{x}_k, y_k, \dot{y}_k)^{\mathrm{T}}$ includes the position vector $(x_k, y_k)^{\mathrm{T}}$ and the velocity vector $(\dot{x}_k, \dot{y}_k)^{\mathrm{T}}$ of the extended target.

The PHD filter is usually used for dealing with the multi-target tracking problem with the dynamic model and measurement model above-mentioned, since it has the ability of avoiding the complicated data association between targets and measurements. The PHD referring to a density function $D_{k|k}(\boldsymbol{x}|\boldsymbol{Z}_k)$, which is also known as an intensity function or a fist-order statistics moment of the RFS [2], is defined as

$$D_k(\boldsymbol{x}) = \int \delta_{\boldsymbol{X}}(\boldsymbol{x})\pi(\boldsymbol{X})\mathrm{d}\boldsymbol{X} \tag{3}$$

where $\pi(\boldsymbol{X})$ is the multi-target density of the RFS.

Let $D_{k-1|k-1}(\boldsymbol{x}|\boldsymbol{Z}_{k-1})$ be the PHD at time-step $k-1$ and $b_{k|k-1}(\boldsymbol{x})$ be the PHD of new-born target. Without taking spawning target into account, the predicted PHD would be calculated as

$$D_{k|k-1}(\boldsymbol{x}|\boldsymbol{Z}_{k-1}) =$$

$$\int f_{k|k-1}(\boldsymbol{x}|\boldsymbol{x}')D_{k-1|k-1}(\boldsymbol{x}'|\boldsymbol{Z}_{k-1})\mathrm{d}\boldsymbol{x}' + b_{k|k-1}(\boldsymbol{x}). \tag{4}$$

On the basis of the Poisson multiple target measurement model [1], the corrector equation for the extended target PHD filter is

$$D_{k|k}(\boldsymbol{x}|\boldsymbol{Z}_k) = L_{\boldsymbol{Z}}(\boldsymbol{x})D_{k|k-1}(\boldsymbol{x}|\boldsymbol{Z}_{k-1}). \tag{5}$$

The equation above denotes that, the posterior PHD intensity is calculated by the product of likelihood function and predicted intensity, where $L_{\boldsymbol{Z}}(\boldsymbol{x})$ denotes the measurement likelihood function. If $\boldsymbol{Z} = \varnothing$, there is

$$L_{\boldsymbol{Z}}(\boldsymbol{x}) = 1 - (1 - \mathrm{e}^{-\gamma(\boldsymbol{x})})P_D(\boldsymbol{x}), \tag{6}$$

otherwise,

$$L_{\boldsymbol{Z}}(\boldsymbol{x}) = 1 - (1 - \mathrm{e}^{-\gamma(\boldsymbol{x})})P_D(\boldsymbol{x}) +$$

$$\mathrm{e}^{-\gamma(\boldsymbol{x})}P_D(\boldsymbol{x}) \sum_{p \angle \boldsymbol{Z}_k} \omega_p \sum_{\boldsymbol{W} \in p} \frac{\gamma(\boldsymbol{x})^{|\boldsymbol{W}|}}{d_{\boldsymbol{W}}} \cdot \prod_{\boldsymbol{z} \in \boldsymbol{W}} \frac{\varphi_z(\boldsymbol{x})}{\lambda_k c_k(\boldsymbol{z}_k)}. \tag{7}$$

The first term of the RHS (right-hand side) of the equation handles the targets where there are no detections, whereas the second term of the RHS handles targets where there are at least one detection. Here, the numbers of

measurements produced by each extended target per sampling time obey Poisson distribution, and the Poisson parameter is $\gamma(\boldsymbol{x})$. According to the Poisson distribution theory, note that $\mathrm{e}^{-\gamma(\boldsymbol{x})}$ is the probability that a target generates no detections. Thus, $1-\mathrm{e}^{-\gamma(\boldsymbol{x})}$ is the probability that contributes at least one detection. As a consequence, $(1-\mathrm{e}^{-\gamma(\boldsymbol{x})})P_D(\boldsymbol{x})$ is the effective probability of detection with the probability of sensor detection $P_D(\boldsymbol{x})$. The clutter distribution is modeled by $\lambda_k c_k(\boldsymbol{z}_k)$, and the notation $\varphi_{z_k}(\boldsymbol{x}) = p(\boldsymbol{z}_k|\boldsymbol{x})$ means the likelihood function measuring the similarity degree between state $\boldsymbol{x}$ and its measurements.

Here, the notation $p\angle\boldsymbol{Z}_k$ indicates that measurement set $\boldsymbol{Z}_k$ is divided into p partitions, and each partition consists of non-zero cells $\boldsymbol{W}$. A cell contains more than one measurement which can be interpreted as coming from the same target. In (7), the summation of the second part is taken over all partitions p. The weight ω_p of the particular partition is

$$\omega_p = \frac{\prod\limits_{\boldsymbol{W}\in p} d_{\boldsymbol{W}}}{\sum\limits_{p'\angle Z_k}\prod\limits_{\boldsymbol{W}\in p'} d_{\boldsymbol{W}}}. \tag{8}$$

If $\delta_{i,j}$ is the Kronecker delta and $|\boldsymbol{W}|$ denotes the number of elements in $\boldsymbol{W}\subseteq\boldsymbol{Z}_k$, then the weight $d_{\boldsymbol{W}}$ of a cell $\boldsymbol{W}$ is

$$d_{\boldsymbol{W}} = \delta_{|\boldsymbol{W}|,1} + D_{k|k-1}\left[\mathrm{e}^{-\gamma}\gamma^{|\boldsymbol{W}|}P_D\prod_{\boldsymbol{z}\in\boldsymbol{W}}\frac{\varphi_z(\boldsymbol{x})}{\lambda_k c_k(\boldsymbol{z}_k)}\right] \tag{9}$$

where for any function $h(x)$, there is

$$D_{k|k-1}[h] = \int h(\boldsymbol{x})D_{k|k-1}(\boldsymbol{x}|\boldsymbol{Z}_{k-1})\mathrm{d}\boldsymbol{x}. \tag{10}$$

The partitioning has a crucial role in the extended target tracking algorithm, due to more than one measurement stemming from the same target. Meanwhile, accurately partitioning the measurement set effectively contributes to distinguishing different targets. For example, we have a measurement set $\boldsymbol{Z}_k = \{\boldsymbol{z}_k^{(1)}, \boldsymbol{z}_k^{(2)}, \boldsymbol{z}_k^{(3)}\}$ containing three independent elements. Then the partitions of $\boldsymbol{Z}_k$ are

$$p_1 : \boldsymbol{W}_1^1 = \{\boldsymbol{z}_k^{(1)}, \boldsymbol{z}_k^{(2)}, \boldsymbol{z}_k^{(3)}\} \tag{11}$$

$$p_2 : \boldsymbol{W}_1^2 = \{\boldsymbol{z}_k^{(1)}, \boldsymbol{z}_k^{(2)}\}, \boldsymbol{W}_2^2 = \{\boldsymbol{z}_k^{(3)}\} \tag{12}$$

$$p_3 : \boldsymbol{W}_1^3 = \{\boldsymbol{z}_k^{(1)}, \boldsymbol{z}_k^{(3)}\}, \boldsymbol{W}_2^3 = \{\boldsymbol{z}_k^{(2)}\} \tag{13}$$

$$p_4 : \boldsymbol{W}_1^4 = \{\boldsymbol{z}_k^{(2)}, \boldsymbol{z}_k^{(3)}\}, \boldsymbol{W}_2^4 = \{\boldsymbol{z}_k^{(1)}\} \tag{14}$$

$$p_5 : \boldsymbol{W}_1^5 = \{\boldsymbol{z}_k^{(1)}\}, \boldsymbol{W}_2^5 = \{\boldsymbol{z}_k^{(2)}\}, \boldsymbol{W}_3^5 = \{\boldsymbol{z}_k^{(3)}\} \tag{15}$$

where, p_i is the ith partition, and $\boldsymbol{W}_j^i$ is the jth cell in the partition. It can be inferred from the above partitioning rules that the number of probable partitions will increase dramatically along with the growing number of elements in the measurement set. In order to reduce the computation complexity, a few reasonable partitions would be taken into account. In this paper, we choose the most suitable partition in calculation by using the strategy of Mahalanobis distance between the two measurements [4].

3. Background

This section gives a brief introduction of the interval analysis and the BPF.

3.1 Interval analysis

A classical real interval, $[x] = [\underline{x}, \overline{x}]$ is a closed and connected subset of the real number. The notations $\underline{x}$ and $\overline{x}$ mean the minimum and the maximum value of a quantity x, respectively. An interval is used for describing a quantity in the presence of a bounded error. Here, both a state and a measurement are affected by uncertainty in the state place, then we introduce the main concept of the interval to represent particles not as points but as boxes to describe the state and measurement with maximum boundary of error. Understandably, the operator $||[\cdot]||$ means the volume of a box $[\cdot]$, and the center of the box would be $\mathrm{mid}([\cdot])$. More details about interval analysis are shown in [8].

3.2 BPF

Traditional measurements are often described by so-called point measurements, while in the real applications, especially in the complicated distributed observing system, it is more reasonable that interval analysis is used to cope with the non-traditional measurements, due to unknown system delay, bounded bias and unexpected synchronization offset. The key idea of the BPF is to approximate the posterior PDF with weighted rectangular region particles in the state place instead of point particles. Using box-particles to represent interval measurements with the maximum error boundary not only can reduce the requirement of the measurements' distribution, but also can avoid distinguishing the measurements originating from the true targets or clutters. Furthermore, we can divide the observation region into arrayed rectangular regions to mark the measurements falling into the range, so that it will greatly simplify the complexity of the system in a complex scenario. More details about the BPF are shown in [8].

4. LBP-CPHD filter for multiple extended targets

The key idea and the details of ET-LBP-CPHD filter are given in this section.

4.1 Main idea

In the ET-BP-PHD filter, state corresponds to measurement at the set level, and the specific links between state estimation and individual target cannot be obtained. In our ET-LBP-CPHD filter, we add a label to each box-particle which records the target identity and can be inherited along with the box-particle evolution procedure, so we can tell which target one box-particle comes from. In this way, state estimation can be obtained by weighting averaging of box-particles with the same label. The difference of state estimation between two methods is shown in Fig. 1.

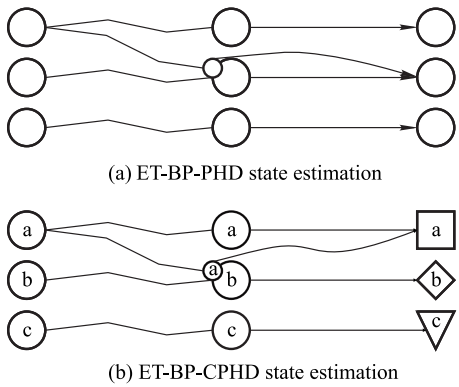

(a) ET-BP-PHD state estimation

(b) ET-BP-CPHD state estimation

Fig. 1 State estimation of ET-BP-CPHD and ET-LBP-CPHD

Fig. 1 shows that in BP-CPHD state estimation, the clustered box-particle set is unrecognized, so the state estimation can only be represented by the same icon ($\bigcirc$). In our LBP-CPHD state estimation, only box-particles with the same label will be associated. Therefore, the estimated state can inherit the label so that we can know which target each estimated state originates from. In this way, individual state estimation is associated with individual target and different targets can be represented with different icons ($\square, \Diamond, \triangledown$), which means the tracks can be discriminated.

Furthermore, if the estimated number of targets is incorrect, multiple states estimation given by standard clustering technique will be unreliable. In the LBP-CPHD filter, the box-particles with the same label are divided into one set, and each labeled box-particle subset corresponds to an individual target. Therefore, the state estimation can be obtained by the weighted average of the box-particles in each subset and avoid clustering.

Another difference between the ET-LBP-CPHD filter and the ET-BP-PHD filter is that the former introduces the recursion of the label and the cardinality distribution. Unlike the targets number gained directly by the sum of the weights of box-particles, the targets number in the ET-LBP-CPHD filter is estimated by the updated cardinality distribution. Because the cardinality distribution is corrected by the measured box-particles, the ET-LBP-CPHD filter can achieve a better performance of number estimation.

4.2 Algorithm

The proposed ET-LBP-CPHD filter has the following steps.

4.2.1 Partitioning the measurement set

Measurements of an extended target belong to an extended region after partition. Using box-particle to replace traditional multiple measurements is exactly suitable to deal with extended targets, without distinguishing the measurements originating from the true targets or clutters.

Here, a simple but effective heuristic approach is used to find an appropriate subset of partitions, which is based on the distance between the measurements [4]. Because the BPF does not distinguish the measurements derived from targets or clutters, we can construct the cells we have received into regular boxes by using the inclusion function $[f]$.

$$[\boldsymbol{zp}_k^{(j)}] = \{[f]\ (\boldsymbol{W}_j)\}, \quad j = 1, \ldots, m_k \tag{16}$$

where, m_k is the number of above-mentioned cells resulting from the partitioning, and the size of the boxes is defined by the spatial extent of the measurements in cells.

Furthermore, the subpartition strategy is adopted when the targets are close to each other and the number in a cell is beyond the threshold χ. In this paper, the subpartition method has the following steps: (i) compute the cluster centers of the measurements in the particular cell, (ii) subdivide the cell into smaller cells according to the spatial extent of the measurements, (iii) extend each smaller cell to a box whose size keeps the same size before subpartition.

4.2.2 Initialization

Assume that the survival box-particle set gained from the previous resampling step is denoted by $\{(l_{k-1}^{per,(i)}, w_{k-1}^{per,(i)}, [\boldsymbol{x}_{k-1}^{per,(i)}])\}_{i=1}^{N}$, $w_{k-1}^{per,(i)}$ and $[\boldsymbol{x}_{k-1}^{per,(i)}]$ represent the corresponding weight and state of the ith box-particle. $l_{k-1}^{per,(i)} \in \Theta_{k-1}^{per} = \{\theta_1, \theta_2, \ldots, \theta_{M_{k-1}}\}$ $(\theta_n \neq 0)$ is the label added to the ith box-particle, where θ_n records the target identity and $\theta_{M_{k-1}}$ is the maximum target identity at time $k-1$, and the cardinality distribution would be achieved as $p_{k-1}(n)$. The information of the newborn target, which lacks the prior knowledge, needs to be sampled in the whole observation region. However, the approach is clearly complex and inefficient. In many practical applications, there is a high possibility that new target will be born in the region of the position of previous measurements [9]. Under the above assumption, the newborn box-particle set $\{(l_{k-1}^{bir,(m)} = 0, w_{k-1}^{bir,(m)}, [\boldsymbol{x}_{k-1}^{bir,(m)}])\}_{m=1}^{N_b}$ is produced

by previous results of the partitioned measurement set. $l_{k-1}^{bir,(m)} = 0$ means the source of the mth box-particle is tentative and needs further processing. Given m_{k-1} being the number of the partition cells in the time step $k-1$, then, for each of the cell we sample

$$N_b^{(j)} = \lceil N_b/m_{k-2} \rceil, \quad j = 1, \ldots, m_{k-2} \tag{17}$$

where $\lceil \cdot \rceil$ denotes the round down operator, and the probability of target birth is P_b. Thus, the weights of the newborn box-particles are assigned,

$$w_{k-1}^{bir,(m)} = P_b/N_b. \tag{18}$$

The whole box-particle set we resample at the initialization step is

$$\begin{aligned} &\{(l_{k-1}^{(i)}, w_{k-1}^{(i)}, [\boldsymbol{x}_{k-1}^{(i)}])\}_{i=1}^{N'} = \\ &\{(l_{k-1}^{per,(i)}, w_{k-1}^{per,(i)}, [\boldsymbol{x}_{k-1}^{per,(i)}])\}_{i=1}^{N} \cup \\ &\{(l_{k-1}^{bir,(m)}, w_{k-1}^{bir,(m)}, [\boldsymbol{x}_{k-1}^{bir,(m)}])\}_{m=1}^{N_b} \end{aligned} \tag{19}$$

where the numbers of the box-particles are $N' = N + N_b$ and $l_{k-1}^{(i)} \in \Theta_{k-1}^{per} \cup \{0\}$.

4.2.3 Time update

The time update step includes weights and cardinality distribution prediction. The box-particles we have got in the initialization step are propagated through the evolution model and the weights of those are predicted by the survival probability $P_S(\cdot)$, i.e.,

$$[\boldsymbol{x}_{k|k-1}^{(i)}] = [f_{k|k-1}]([\boldsymbol{x}_{k-1}^{(i)}]), \quad i = 1, \ldots, N' \tag{20}$$

$$w_{k|k-1}^{(i)} = P_S([\boldsymbol{x}_{k-1}^{(i)}]) w_{k-1}^{(i)}, \quad i = 1, \ldots, N'. \tag{21}$$

Meanwhile, the cardinality distribution, which also contains high-order information of the targets number, is propagated by a "transfer matrix" $\boldsymbol{M}$:

$$p_{k|k-1}(n) = \sum_{n'=0}^{\infty} p_{k-1}(n') \boldsymbol{M}(n, n') \tag{22}$$

$$\boldsymbol{M}(n, n') = \sum_{i=0}^{\min\{n, n'\}} p_{bir}(n-i) \binom{n'}{i} d^{n'-i} (1-d)^i \tag{23}$$

where, $p_{bir}(n)$ is the probability for n targets to newly appear from the time step $k-1$ to k through the target birth model. And, d denotes the probability of target "death", which is $d = 1 - P_S(\cdot)$. For a constant scan rate, the so-called Markov transition matrix $\boldsymbol{M}$ is a constant and could be computed in advance. It is clear that the matrix $\boldsymbol{M}$ is relying on the newborn cardinality distribution probability $p_{bir}(n)$ and the death probability d. In other words, the LBP-CPHD filter is more heavily influenced by its underlying motion model for target birth and death. Owing to the two mentioned models which are always stable and reliable, the cardinality propagation in the LBP-CPHD filter has an excellent memory.

4.2.4 Measurement update

The implementation of the box-particles' state update requires to calculate the likelihood function, so does the cardinality distribution update. In fact, the two updated steps are coupled with each other. The equation of the box-particles states and weights update are as follows:

$$[\boldsymbol{x}_k^{(i)}] = [h_{cp}]([\boldsymbol{x}_{k|k-1}^{(i)}], [\boldsymbol{z}\boldsymbol{p}_k^{(j)}]), \quad i = 1, \ldots, N' \tag{24}$$

$$\begin{aligned} w_k^{(i)} &= (1 - P_D) \frac{L([\boldsymbol{Z}_k]|\neg D)}{L([\boldsymbol{Z}_k])} w_{k|k-1}^{(i)} + \\ &P_D \frac{L([\boldsymbol{Z}_k]|D)}{L([\boldsymbol{Z}_k])} w_{k|k-1}^{(i)}, \quad i = 1, \ldots, N' \end{aligned} \tag{25}$$

where P_D denotes the probability of sensor detection. D and $\neg D$ are the short hand notations for targets detected and not detected, respectively. The first term of the RHS represents the weights update in case of no targets detected by the sensor. On the contrary, the second term of the RHS denotes the weights update for detected. Unlike the BP-PHD filter correcting the weights only for the detected targets, the BP-CPHD filter updates the weights of the missing detected targets as well as the detected ones. So the latter filter shows its delay characteristics to the upcoming measurements and will achieve more stable and precise estimation in the case of missing detection. However, the BP-CPHD filtering will tend to respond sluggishly for the new arrived measurements, especially when the targets disappear, so that the filter would produce time delay on the number estimation, which is also an inherent drawback of CPHD-type filters.

The measurement update equation of the cardinality distribution is implemented as

$$p_k(n) = \frac{L([\boldsymbol{Z}_k]|n)}{L([\boldsymbol{Z}_k])} p_{k|k-1}(n). \tag{26}$$

For multiple extended targets tracking, the likelihood function in the BP-CPHD filter has the similar form as that in the BP-PHD filter. The proposed BP-CPHD filter updates the cardinality distribution through the likelihood function.

$$l_k([\boldsymbol{z}\boldsymbol{p}_k^{(j)}]|[\boldsymbol{x}_{k|k-1}^{(i)}]) = \frac{|[h_{cp}]([\boldsymbol{x}_{k|k-1}^{(i)}], [\boldsymbol{z}\boldsymbol{p}_k^{(j)}])|}{|[\boldsymbol{x}_{k|k-1}^{(i)}]|} \tag{27}$$

$$[h_{cp}]([\boldsymbol{x}_{k|k-1}^{(i)}], [\boldsymbol{z}\boldsymbol{p}_k^{(j)}]) = [\boldsymbol{x}_{k|k-1}^{(i)}] \cap [\boldsymbol{z}\boldsymbol{p}_k^{(j)}] \tag{28}$$

where h_{cp} is the contract propagation algorithm. Here, the contractor is constructed by the overlapping area between the predicted and the corresponding measurement box-particles.

$$L([\boldsymbol{Z}_k]|\neg D) =$$

$$\frac{1}{n_{k|k-1}}\sum_{j=0}^{m_k}\alpha^{(j+1)}\beta^{(j)}\sigma_j(\{L_k^{(1)},\dots,L_k^{(m_k)}\}) \tag{29}$$

$$L([\boldsymbol{Z}_k]|D)=\sum_{j=1}^{m_k}l([\boldsymbol{zp}_k^{(s)}]|[\boldsymbol{x}])L([\boldsymbol{Z}_k]|a_k^{(j)}=s) \tag{30}$$

$$L([\boldsymbol{Z}_k]|a_k^{(j)}=s)=\frac{1}{n_{k|k-1}}\times$$

$$\sum_{j=1}^{m_k}\beta_k^{(j)}\alpha_k^{(j)}\sigma_{j-1}\times(\{L_k^{(1)},\dots,L_k^{(m_k)}\}/\{L_k^{(s)}\}) \tag{31}$$

$$L([\boldsymbol{Z}_k])=\sum_{j=0}^{m_k}\alpha^{(j)}\beta^{(j)}\sigma_j(\{L_k^{(1)},\dots,L_k^{(m_k)}\}) \tag{32}$$

$$L([\boldsymbol{Z}_k]|n)=\sum_{j=0}^{\min(m,n)}\beta_k^{(j)}\frac{n!}{(n-j)!}(1-P_D)^{n-j}\times$$

$$\sigma_j(\{L_k^{(1)},\dots,L_k^{(m_k)}\}) \tag{33}$$

$$L_k^{(s)}=\frac{1}{n_{k|k-1}}\times\int P_D w_{k|k-1}([\boldsymbol{x}])l_k([\boldsymbol{zp}_k^{(s)}]|[\boldsymbol{x}])\mathrm{d}[\boldsymbol{x}] \tag{34}$$

$$\alpha^{(j)}\equiv\sum_{n=j}^{\infty}\frac{n!}{(n-j)!}p_{k|k-1}(n)(1-P_D)^{n-j} \tag{35}$$

$$\beta_k^{(j)}\equiv p_c(m-j)\frac{(m_k-j)!}{m_k!}\lambda^{-j} \tag{36}$$

where $p_c(m)$ denotes the probability for m false alarms exist. And the elementary symmetric function $\sigma_j(\cdot)$ can be calculated as

$$\sigma_j(\{y_1,\dots,y_m\})=\sum_{1\leqslant i_1<\cdots<i_j\leqslant m}y_{i_1}y_{i_2}\cdots y_{i_j} \tag{37}$$

with $\sigma_0\equiv 1$.

After the prediction and update of the cardinality distribution, the BP-CPHD filter propagates the complete information of targets number, and could precisely track the real-time change in number of targets.

4.2.5 Box-particles contraction

For the extended targets tracking, a box-particle is a nonzero rectangular region representing the irregular predicted extent or measured partition cell, which itself contains some redundant information. Also, a box converted by the nonlinear motion model and inclusion function would definitely covers redundant parts. In order to reduce the redundant information, the contraction step is introduced. Moreover, each box-particle is contracted with its corresponding measurement, which is defined as follows:

$$[\boldsymbol{z}_k]=\arg\max_{w_{j,i}}\{[\boldsymbol{zp}_k^{(j)}],w_{j,i}>0\} \tag{38}$$

$$w_{j,i}=P_D\frac{L([\boldsymbol{Z}_k]|D)}{L([\boldsymbol{Z}_k])}. \tag{39}$$

If no such $[\boldsymbol{z}_k]$ is found, this particle needs not to be contracted; otherwise, it needs to be contracted according to the corresponding predicted box-particle and measured box we obtained:

$$[\widetilde{\boldsymbol{x}}_k^{(i)}]=[h_{cp}]([\boldsymbol{x}_k^{(i)}],[\boldsymbol{z}_k]). \tag{40}$$

4.2.6 Number estimation

Generally speaking, we can adopt either expected a posteriori (EAP) method or maximum a posteriori (MAP) method to estimate the number of targets.

The EAP estimation works as follows:

$$\widehat{N}_k=\sum_{n=0}^{\infty}np_k(n). \tag{41}$$

The MAP estimation works as follows:

$$\widehat{N}_k=\arg\max_n p_k(n). \tag{42}$$

The MAP estimation [2] often produces stable and accurate posterior expected number-estimation under lower-SNR conditions, so the MAP estimation method is selected in this paper to evaluate target number.

4.2.7 Label update

Label processing is based on the assumption: the target disappears and is newborn not at the same time. Under this assumption, label processing is divided into three cases:

(i) When the estimated number at time k is greater than the estimated number at the previous moment, that is, $\widehat{N}_k>\widehat{N}_{k-1}$, it is shown that the newborn target is detected in the newborn box-particles, and the number of newborn targets is $\widehat{N}_{k,\mathrm{new}}=\widehat{N}_k-\widehat{N}_{k-1}$. Then update the labels of $\widehat{N}_{k,\mathrm{new}}$ maximum weight box-particles with label 0, respectively, to $(\theta_{M_{k-1}}+1),\dots,(\theta_{M_{k-1}}+\widehat{N}_{k,\mathrm{new}})$, and θ_{M_k} can be updated as $\theta_{M_k}=\theta_{M_{k-1}}+\widehat{N}_{k,\mathrm{new}}$.

(ii) When $\widehat{N}_k=\widehat{N}_{k-1}$, it indicates that there is no newborn target detected in newborn box-particles. The labels remain unchanged.

(iii) When $\widehat{N}_k<\widehat{N}_{k-1}$, it means that one or more targets have disappeared. At this point, compare the weights of each target calculated in (45) with the threshold η. If

the weight of a target is less than the threshold, the target disappears and the corresponding label is changed to 0.

$$\widehat{w}_k^{\theta_n} = \sum_{i=\widetilde{N}_k^{\theta_{n-1}}+1}^{\widetilde{N}_k^{\theta_n}} w_k^{(i)} \tag{43}$$

$$\widetilde{N}_k^{\theta_n} = \sum_{j=0}^{n}\sum_{i=1}^{N_k}\delta(l_k^{(i)}-\theta_j), \quad \theta_0 = \varnothing \tag{44}$$

$$\theta_n = \begin{cases} 0, & \widehat{w}_k^{\theta_n} < \eta \\ \theta_n, & \text{otherwise} \end{cases}. \tag{45}$$

After label processing, label 0 means clutter, so we empty the label 0 set $\{\theta_j | \theta_j = 0, j = 0,1,2,\ldots,M_k\} = \varnothing$, then the updated label set is $l_k^{(i)} \in \Theta_k = \{\theta_1, \theta_2, \ldots, \theta_{M_k}\}$.

4.2.8 State estimation

The box-particles with the same label come from the same target, so we divide the box-particles with the same label into a set $P_k^{\theta_n} = \{(l_k^{(i)} = \theta_n, w_k^{(i)}, [\boldsymbol{x}_k^{(i)}])\}_{i=1}^{N'}$. Then $P_k^l = P_k^{\theta_1} \cup \cdots \cup P_k^{\theta_{M_k}}$, and multi-target estimation is changed into multiple single target estimation.

As shown in Fig. 2, each non-zero label corresponds to one target, so the state of target n can be obtained by weighting averaging the set $P_k^{\theta_n}$:

$$\widehat{\boldsymbol{x}}_{\theta_n} = \frac{1}{\widehat{w}_k^{\theta_n}} \sum_{i \in P_k^{\theta_n}} \text{mid}([\boldsymbol{x}_k^{(i)}]) \cdot w_k^{(i)}. \tag{46}$$

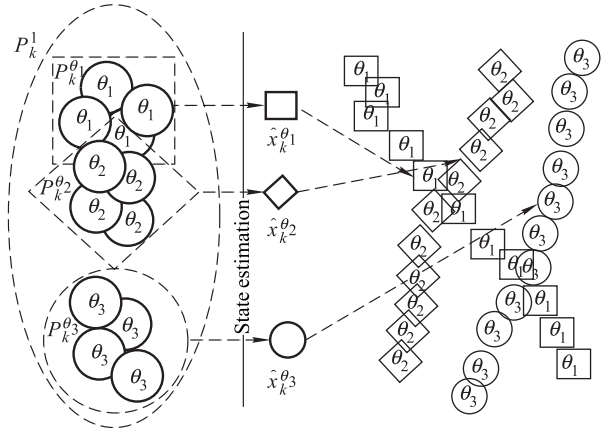

Fig. 2 ET-LBP-CPHD state estimation

4.2.9 Resampling

Different from the resample strategy of just replicating particles according to the number which they have been chosen in particle filter, we divide the estimated box-particle into smaller sub-box-particles as many as they are selected in the resampling step [7]. The subdivision strategy can not only satisfy the requirements in the next time step, but also increase the variety of the box-particles. However, in contrast to other particles, the degeneracy of box-particles is not only the degeneracy of their weights and diversity but also the degeneracy of information. Therefore, we add an information supplemental step after resampling the LBP-CPHD filter.

In this paper, by means of parallel resampling each labeled box-particle set $P_k^{\theta_n}(\theta_n \in \Theta_k)$, we can resample each target separately. Assuming that the number of resampling per target is N_{box}, the labeled box-particle set $P_k^{\theta_n}$ for resampling target labeled θ_n is

$$P_k^{\theta_n} = \{(l_k^{(i)} = \theta_n, w_{k-1}^{(i)} = 1/N_{\text{box}}, [\boldsymbol{x}_{k-1}^{(i)}])\}_{i=1}^{N_{\text{box}}}. \tag{47}$$

After resampling $\widehat{N}_k$ targets, the new box-particle set is $P_k^l = \{(l_k^{(i)}, w_{k-1}^{(i)}, [\boldsymbol{x}_{k-1}^{(i)}])\}_{i=1}^{N_k}$, where $N_k = \widehat{N}_k \cdot N_{\text{box}}$.

5. Simulation results

This section demonstrates numerical studies to evaluate the performance of the proposed ET-LBP-CPHD filter and to compare with the ET-BP-PHD filter and the ET-BP-CPHD filter. In the simulation, the optimal subpattern assignment (OSPA) distance and the cardinality are applied as performance evaluation criteria.

Considering a 2-D surveillance region $A = [-400, 400] \times [-500, 500]\ \text{m}^2$ with random clutters, there locate several targets with a time-varying number. The clutters are modeled as a Poisson RFS with the mean r per scan over the surveillance region. Without loss of generality, the system dynamic model and the measurement model are the interval form as follows:

$$[\boldsymbol{x}_k] = \boldsymbol{F}[\boldsymbol{x}_{k-1}] + \boldsymbol{G}[u_{k-1}] \tag{48}$$

$$[\boldsymbol{z}_k] = \boldsymbol{H}[\boldsymbol{x}_k] + [\upsilon_k] \tag{49}$$

$$[\boldsymbol{x}_k] = [[x_k], [\dot{x}_k], [y_k], [\dot{y}_k]]^{\text{T}} \tag{50}$$

$$[\boldsymbol{z}_k] = [x_k, y_k]^{\text{T}} \tag{51}$$

$$[\boldsymbol{zp}_k] = [[xp_k], [yp_k]]^{\text{T}} \tag{52}$$

where the targets are moving according to the nearly constant velocity (CV) motion model with the parameter matrix:

$$\boldsymbol{F} = \begin{bmatrix} 1 & T & 0 & 0 \\ 0 & 1 & 0 & 0 \\ 0 & 0 & 1 & T \\ 0 & 0 & 0 & 1 \end{bmatrix}, \quad \boldsymbol{G} = \begin{bmatrix} T^2/2 & 0 \\ T & 0 \\ 0 & T^2/2 \\ 0 & T \end{bmatrix},$$

$$\boldsymbol{H} = \begin{bmatrix} 1 & 0 & 0 & 0 \\ 0 & 0 & 1 & 0 \end{bmatrix} \tag{53}$$

with sampling time $T = 1$. Here, the kinematic state vector is in the form $[\boldsymbol{x}_k] = [[x_k], [\dot{x}_k], [y_k], [\dot{y}_k]]^{\text{T}}$, consisting

of the position interval vector $[[x_k],[y_k]]^{\mathrm{T}}$ and the velocity interval vector $[[\dot{x}_k],[\dot{y}_k]]^{\mathrm{T}}$. The measurements of an extended target are distributed as a Gaussian with their center being the true location, and the mean number of measurements generated by one extended target is Poisson distribution with $\lambda_T = 10$. Besides, the interval form $[\boldsymbol{zp}_k]$ denotes the box containing measurement partition cells. The interval is formed according to the 3σ rule. Here, $\omega_{k-1}$and υ_k are process noise and measurement noise, respectively, and they both are zero mean white Gaussian. The standard deviations for x and y coordinates of the process noise $\sigma_x = \sigma_y = 0.1$ and the measurement noise $\widetilde{\sigma}_x = \widetilde{\sigma}_y = 0.5$ are fixed. Given that the probability of target survival is $P_S = 0.99$ and the newborn probability is $P_b = 0.01$, the parameters of the OSPA distance are set to $p = 2$ and $c = 70$. What is more important in the presented filter, the width and height of the box-particles initialized are both set at 25. In both compared filters, each target is assigned 50 box-particles as survival box-particles, and 3 newborn box-particles are supplemented for every partition cell according to measurement partition results in the previous time step.

The initial state and moving duration of the targets are shown in Table 1.

Table 1 Initial state and moving duration

Target label	Initial state/ (m, m/s, m, m/s)	Start time/s	End time /s
1	(50, 0, 400, −15)	1	40
2	(−50, 13, 80, −10)	6	34
3	(−100, 12, −300, 20)	10	30
4	(−200, 14, −40, 26)	13	27

The true target trajectories and the simulation results for one Monte Carlo trial are demonstrated in Fig. 3.

The advantage of the ET-LBP-CPHD filter that can distinguish tracks can be observed from Fig. 3, where in ET-LBP-CPHD filter, four different targets can be represented with four different icons, while the other two methods can only represent different targets with the same icon.

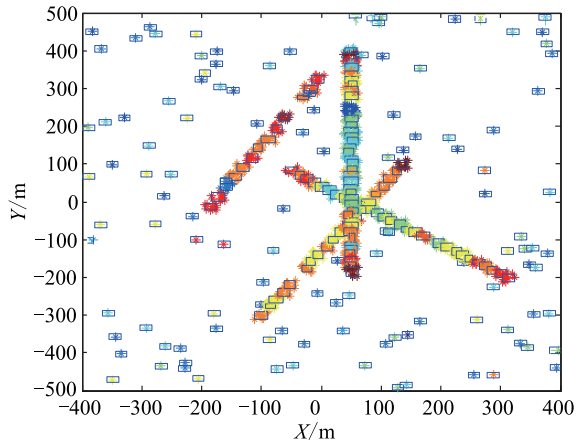

(a) Measurements

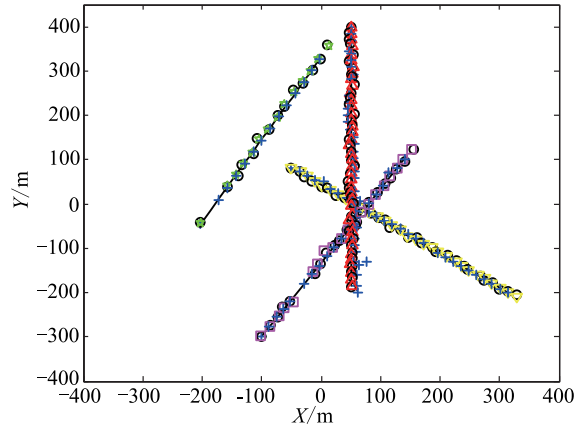

(b) Target trajectory

△ : ET-LBP-CPHD track 1; ▽ : ET-LBP-CPHD track 2;
□ : ET-LBP-CPHD track 3; ☆ : ET-LBP-CPHD track 4;
+ : ET-BP-PHD tracks; ○ : ET-BP-CPHD tracks.

Fig. 3 Target trajectories and position estimate of the three filters mentioned

Fig. 4 and Fig. 5 show the average performance over 50 Monte Carlo runs for the three mentioned filters in the condition of high probability of detection over the scan. At the first sight of the two figures, we could find that both the ET-LBP-CPHD filter and the ET-BP-CPHD filter have a better performance than the ET-BP-PHD filter.

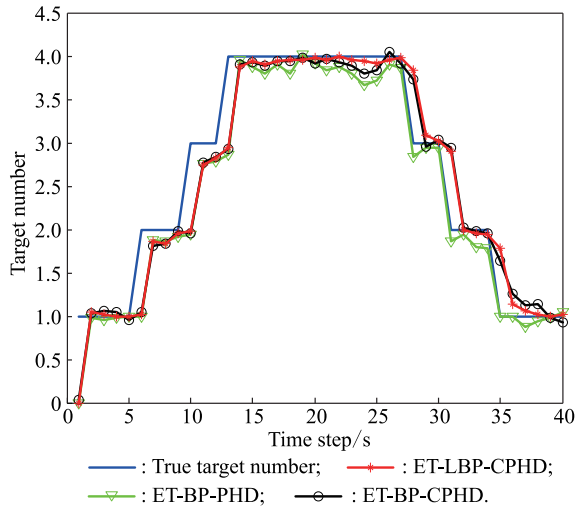

Fig. 4 Mean estimate number of targets for 50 Monte Carlo trials with the probability of detection $P_D = 0.95$ and the mean number of clutter $r = 3$ for three filters

From Fig. 4, when a new target birth (6 s, 10 s, 13 s in Fig. 4), a time step of a missed detection is shown for all BP-type filters, since there are no corresponding predicted box-particles supplemented by previous measurements to detect the new target. It is reasonable to appear a time delay in theory, which could be also easily observed from the OSPA distance in Fig. 5. When a target disappears, the number estimation for both the ET-LBP-CPHD filter and

the ET-BP-CPHD filter do not response immediately, but with a certain delay (27 s, 30 s, 34 s) demonstrated in Fig. 4. It is because target death can be regarded as a missed detection at the time, while the two CPHD based filters have the characteristic to respond sluggishly in a missed detection case. On the contrary, the ET-BP-PHD filter responds sharply to new measurements due to its bad memory, so the number of targets decreases immediately.

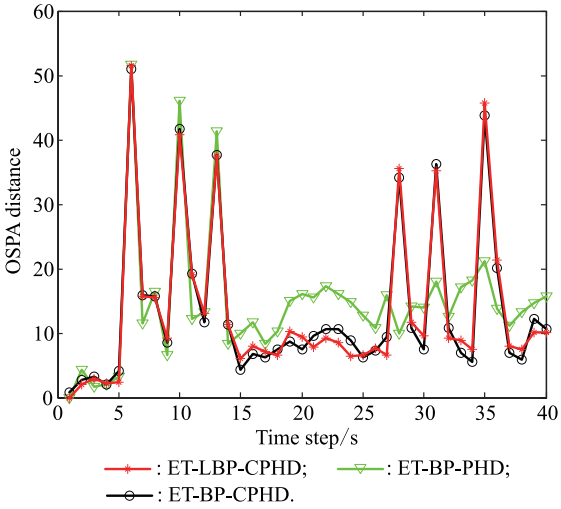

Fig. 5 Mean OSPA distance value for 50 Monte Carlo trials with the probability of detection $P_D = 0.95$ and the mean number of clutter $r = 3$ for three filters

Owing to an accurate partition result while only a few targets exist and are far from each other, the measured box-particles used to update contain less uncertainty. When there is no disappeared target, the ET-LBP-CPHD filter and the ET-BP-CPHD filter have a better advantage over the ET-BP-PHD filter on estimating number. The reasons can be summarized as follows: (i) The ET-LBP-CPHD filter and the ET-BP-CPHD filter propagate the cardinality distribution, which contains the high-order information of the targets number and can be more precise to obtain the number of targets. (ii) Number estimation of the ET-LBP-CPHD filter and the ET-BP-CPHD filter is more heavily influenced by the underlying motion models for birth and death, which could be set in advance in the simulation, so the filter is more stable and robust than the ET-BP-PHD filter. (iii) The two CPHD based filters update with the detected parts and also non-detected parts, bringing the characteristics to respond sluggishly in a missed detection case. In a word, the ET-LBP-CPHD filter and the ET-BP-CPHD filter are more effective to evaluate the number of targets especially in the condition of a missed detection than the ET-BP-PHD filter. The performances of the ET-LBP-CPHD filter and ET-BP-CPHD filter are nearly the same, because the ET-LBP-CPHD algorithm does not change the structure of the CPHD filter except adding labels.

Fig. 6 and Fig. 7 show the average performance over 50 Monte Carlo runs for the two mentioned filters with the same clutter parameter while lower detection probability $P_D = 0.90$.

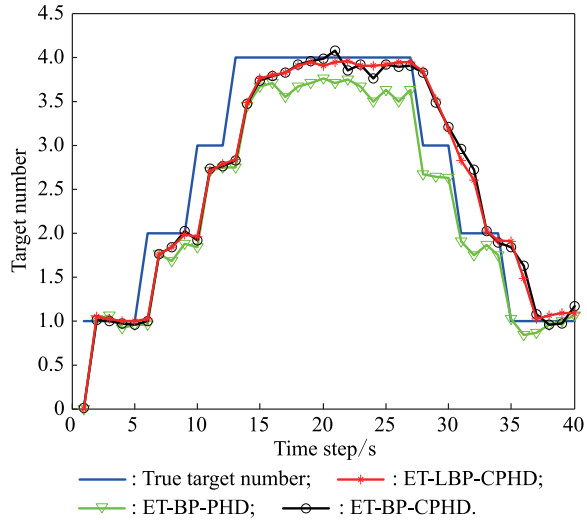

Fig. 6 Mean estimate number of targets for 50 Monte Carlo trials with the probability of detection $P_D = 0.90$ and the mean number of clutter $r = 3$ for three filters

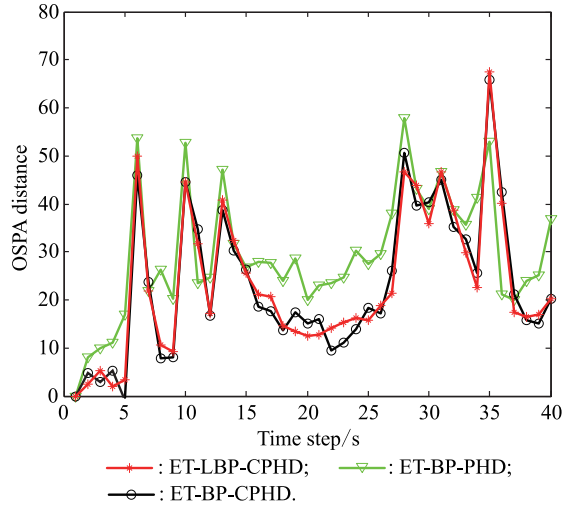

Fig. 7 Mean OSPA distance value for 50 Monte Carlo trials with the probability of detection $P_D = 0.90$ and the mean number of clutter $r = 3$ for three filters

From the comparison of Fig. 4 and Fig. 6, along with the probability of detection decreasing, the precision of the number estimation has been getting worse for the three filters. The probability of detection decreasing means that there exist more missed detections. Compared to the ET-BP-PHD filter, obviously, the ET-LBP-CPHD filter and the ET-BP-CPHD filter perform more stably and robustly owing to the characteristics of time delay and effective memory under the condition of low detection probability.

However, when the detected probability is reduced to a certain level, the three filters work in poor performances with the OSPA distance shown in Fig. 7, because of the fact that box-particles detected are not adequate to approximate the posterior PDF of the filter. In this case, we can improve the performance by increasing the number of box-particles.

6. Conclusions

This paper proposes a labeled box-particle CPHD filter for multiple extended targets tracking. The proposed filter not only inherits the advantages of the box-particle filter dealing with interval measurements in real-time and the CPHD filter propagating high-order information of targets number, but also provide the identity of individual targets. Compared with the ET-BP-PHD filter, the ET-LBP-CPHD filter performs more precise number estimation for multiple extended targets tracking scenario with denser clutters and higher false alarms. Owing to the characteristics of a good memory and the time delay, the ET-LBP-CPHD filter offers more stable estimation in the case of lower detected probability. Compared with the ET-BP-CPHD filter, the proposed filter has similar performance both in number estimation and OSPA distance, while this approach can distinguish different tracks. Numerical simulations show that, it is of positive significance to apply the LBP-CPHD filter into multiple extended targets tracking instead of the BP-PHD filter and the BP-CPHD filter.

References

[1] GILHOLM K, SALMOND D. Spatial distribution model for tracking extended object. Radar, Sonar and Navigation, 2005, 152(5): 364 – 371

[2] MAHLER R. Statistical multisource-multitarget information fusion. Norwood, USA: Aretech House, 2007.

[3] MAHLER R. PHD filters for nonstandard targets, I: extended targets. Proc. of the International Conference on Information Fusion, 2009: 915 – 921.

[4] GRANSTROM K, LUNDQUIST C. A Gaussian mixture PHD filter for extended target tracking. Proc. of the International Conference on Information Fusion, 2010: 1 – 8.

[5] ORGUNER U, LUNDQUIST C, GRANSTROM K. Extended target tracking with a cardinalized probability hypothesis density filter. Proc. of the International Conference on Information Fusion, 2011: 1 – 8.

[6] LIAN F, HAN C Z, LIU W F, et al. Unified cardinalized probability hypothesis density filters for extended targets and unresolved targets. Signal Processing, 2012, 92(7): 1729 – 1744.

[7] ABDALLAH F, GNING A, BONNIFAIT P. Box particle filtering for nonlinear state estimation using interval analysis. Automatica, 2008, 44(3): 807 – 815.

[8] MOORE R E, KEARFOTT R B, CLOUD M J. Introduction to interval analysis. Philadelphia, USA: Society for Industrial and Applied Mathematics, 2009.

[9] GNING A, RISTIC B, MIHAYLOVA L. Bernoulli particle/box-particle filters for detection and tracking in the presence of triple measurement uncertainty. IEEE Trans. on Signal Processing, 2012, 60(5) : 2138 – 2151.

[10] SCHIKORA M, GNING A, MIHAYLOVA L, et al. Box-particle PHD filter for multi-target tracking. Proc. of the International Conference on Information Fusion, 2012: 106 – 113.

[11] SCHIKORA M, GNING A, MIHAYLOVA L, et al. Box-particle probability hypothesis density filtering. IEEE Trans. on Aerospace and Electronic Systems, 2014, 50(3): 1660 – 1672.

[12] SONG L P, ZHAO X G. Box-particle cardinality balanced multi-target multi-Bernoulli filter. Radioengineering, 2014, 23(2): 11 – 15.

[13] PETROV N, GNING A, MIHAYLOVA L. Box particle filtering for extended object tracking. Proc. of International Conference on Information Fusion, 2012: 82 – 89.

[14] PETROV N, ULMKE M, MIHAYLOVA L, et al. On the performance of the box particle filter for extended object tracking using laser data. Proc. of Sensor Data Fusion: Trends, Solutions, Applications, 2012: 19 – 24.

[15] PETROV N, MIHAYLOVA L, GNING A. Rectangular extended object tracking with box particle filter using dynamic Constraints. Proc. of the Data Fusion & Target Tracking: Algorithms & Applications, 2014: 1 – 7.

[16] PETROV N, MIHAYLOVA L, FREITAS D, et al. Crowd tracking with box particle filtering. Proc. of the International Conference on Information Fusion, 2014: 1 – 7.

[17] SONG L P, YAN C, JI H B, et al. PHD filter for tracking multiple extended targets using box particle. Control and Decision, 2015, 30(10): 1759 – 1768. (in Chinese)

[18] SONG L P, LIANG M, JI H B. Box-particle implementation and comparison of cardinalized probability hypothesis density filter. Radioengineering, 2016, 25(1): 177 – 186.

[19] MAHLER R. PHD filters of higher order in target number. IEEE Trans. on Aerospace and Electronic Systems, 2007, 43(4): 1523 – 1543.

[20] JING P L, ZOU J W, DUAN Y, et al. Generalized CPHD filter modeling spawning targets. Signal Processing, 2016, 128: 48 – 56.

[21] ZHU H Y, HAN C Z, LIN Y. Particle labeling PHD filter for multi-target track-valued estimates. Proc. of the International Conference on Information Fusion, 2011: 1 – 8.

[22] LI Y X, XIAO H T, WU H, et al. Labeled particle unresolved target PHD filter for multiple group target tracking. Proc. of the International Radar Conference, 2016: 1 – 5.

Biographies

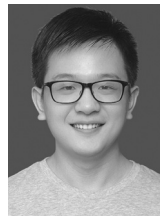

ZOU Zhibin was born in 1994. He is a master degree candidate at the School of Electronic Engineering at Xidian University. His research interests include nonlinear filtering and target tracking.
E-mail: zbzou@stu.xidian.edu.cn

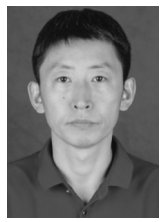

SONG Liping was born in 1975. He received his M.Sc. degree in signal processing from Xidian University in 2003. He received his Ph.D. degree in pattern recognition and intelligent systems from Xidian University in 2008. He is currently an associate professor of Xidian University. His research interests include signal processing, target tracking and nonlinear filtering.
E-mail: lpsong@xidian.edu.cn

CHENG Xuan was born in 1991. He is a master degree candidate at the School of Electronic Engineering at Xidian University. His research interests include box-particle filter and group target tracking. E-mail: chengxuanxd@163.com